



PERFORMANCE ANALYSIS OF SMART ANTENNA BASED ON MVDR BEAMFORMER USING RECTANGULAR ANTENNA ARRAY

Suhail Najm Shahab¹, Ayib Rosdi Zainun¹, Nurul Hazlina Noordin¹, Ahmad Johari Mohamad¹ and Omar Khaldoun A.²

¹Faculty of Electrical and Electronics Engineering, Universiti Malaysia Pahang, Pahang, Malaysia

²School of Computer and Communication Engineering, University Malaysia Perlis, Malaysia

E-Mail: 68suhel@gmail.com

ABSTRACT

The performance of smart antenna system greatly relies on the beam forming technique that forming the main lobe beam pattern to the desired user direction and place null in the direction of undesired interference source. This paper investigates the implementation of Minimum Variance Distortionless Response (MVDR) Adaptive Beam-Forming (ABF) algorithm on Rectangular Antenna Array (RAA) is discussed and analyzed. The MVDR ABF technique performance is studied in accordance with varying the number of array elements, spacing between the array elements, the number of interference sources, noise power label, and the number of snapshots. The MVDR performance is compared on the basis of output radiation pattern and SINR. Computer simulation results show that the performance of the MVDR improved as the number of elements get more. This mean MVDR strongly depends on the number of the element. 0.5λ is considered the best spacing between adjacent antenna elements, the performance degraded as the noise power label increased, and more accurately resolution occurred when the number of snapshots increased.

Keywords: beamforming, minimum variance distortionless response, rectangular antenna array, smart antenna.

INTRODUCTION

Most beam forming techniques have been considered for using at the base station (BS) since antenna arrays are not feasible at mobile terminals due to space limitations [1].

The Long Term Evolution (LTE) as defined by the 3rd Generation Partnership Project (3GPP) is a highly flexible radio interface, its initial deployment of LTE is in 2011. LTE is the evolution of 3GPP Universal Mobile Telecommunication System (UMTS) towards an all-IP network to ensure the competitiveness of UMTS for all next ten years and beyond. LTE was being developed in Release 8 and 9 of the 3GPP specification. According to Maravedis anticipates that 3 LTE-TDD and 59 LTE- FDD networks will be operational worldwide by the end of 2011. There will be 305 million LTE subscribers by 2016, which is about 44 million (14%) will be TDD-LTE users, and the rest 261 million (86%) will be FDD-LTE. [2]. With increasing trend of the number of subscribers and demand for different services in wireless systems, there are always requirements for better coverage, higher data rate, improved spectrum efficiency and reduced operating cost. To fulfill these requirements, beamforming technique able to focus the array antenna pattern into a particular direction and thereby enhances the signal strength.

Interference is one of the significant obstacles in wireless communications. The interference can be caused by the signal itself or by other users [3]. The signal can interfere with itself due to multipath components, where the signal is gathered with another version of the signal that is delayed because of another propagation path. The fundamental principle of ABF is to track the statistics of the surrounding interference and noise field and adaptively search for the optimum location of the nulls that can most significantly reduce the interference and noise under

the constraint that the desired signal is not distorted at the beamformer's output [4].

The basic idea of the MVDR algorithm is to estimates the beamforming coefficients in an adaptive way by minimizing the variance of the residual noise and interference while enforcing a set of linear constraints to ensure that the desired signals are not distorted [4]. The authors in [5] proposed an enhanced model of MVDR algorithm by changing the position of the reference element in steering vector to be in the middle of the array with an odd number of elements. Simulation results showed that modified MVDR has a realistic behavior, especially for detecting the incoming signal's direction and outperforms the conventional MVDR. The signal to interference plus noise ratio (SINR) maximization is one of the criterion employed in joint transmitter and receiver BF algorithms [6, 7]. In [8] mentioned that the element spacing must be $d \leq \lambda/2$ to prevent spatial aliasing. In [9] the author presents a comparative study of minimum variation distortionless algorithm and Least Mean Square (LMS) algorithm. Results indicated that LMS is a better performer.

Smart antennas (SA) include signal processing capabilities that perform tasks such as the direction of arrival (DOA) estimation of a signal and then the SA can adjust the antenna itself using beamforming (BF) techniques to achieve better transmission or reception beam pattern, which increases SINR by mitigating co-channel interference present in wireless communication system. A SA that is held in the BS of a mobile system comprises an array of antennas where the amplitudes are accustomed to a group of complex weights using an adaptive beamforming algorithm. The ABF algorithm improves the output of the array beam pattern in a way that it maximizes the radiated power where it will be produced in the directions of the wanted mobile users. Moreover, deep nulls are



produced in the directions of unwanted signals that symbolize co-channel interference from mobile users in the adjacent cells. Before adaptive beamforming, the direction of arrival estimation is used to specify the main directions of users and interferers. The function of ABF algorithm is used to direct the main beam towards look direction and nulls towards jammer directions.

So far, ABF is a function of the number of element, spacing between adjacent elements, the angular separation between Signal-of-Interest (SOI) and Signal-Not-of-Interest (SNOI), noise power level and number of snapshots. Therefore, it is important to investigate the impact of these parameters on the radiation pattern of an antenna array that able to offer the best BF capabilities in term of directing the main beam toward the direction of the SOI while placing nulls towards the direction of SNOI. This work includes simulation results and performance analysis of MVDR algorithm with rectangular antenna array. The analysis of the MVDR in this work is in four scenarios where the MVDR performance is evaluated with two important metrics; beampattern and SINR. This analysis does not only help us better understand the MVDR beamformer but also help us design better array systems in practical application. The remainder of this paper is organized as follows. In section III, beamformer design method is described. The simulation setup and the numerical outcomes obtained, and discussion are provided in Section IV. At last, Section V concludes the paper.

METHODOLOGY

The mathematical formulation of the design model for adaptive beamforming will be presented in detail in this section. Let there is S desired signal and I interference sources transmitting on same frequency channel simultaneously. The algorithm starts by constructing a real-life signal model. Consider a number of plane waves from K narrowband sources impinging from azimuth and elevation angles (θ, ϕ) , the impinging radio frequency signal reaches into the antenna array from a far field to the RAA geometry. If the interelement distance is constant, it is called Uniform Rectangular Array (URA).

Figure-1 show a rectangular antenna array placed on the x - y plane. There are N elements in the x -direction and M elements in the y -direction creating an $N \times M$ array of identical elements. The n -mth element has weight w_{nm} . The x -directed elements are spaced d_x apart, and the y -directed elements are spaced d_y apart. The rectangular array can be viewed as N linear arrays of M elements or as M linear arrays of N elements.

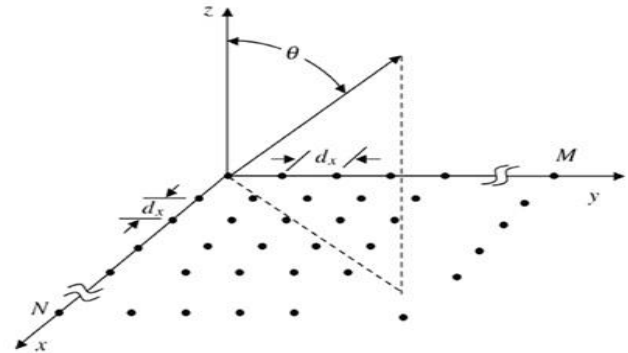


Figure-1. Rectangular antenna array geometry [10].

The total signals received by an adaptive antenna array at time index, t , become:

$$x_T(t) = \sum_{s=1}^S x_s(t) + \sum_{i=1}^I x_i(t) + x_n \quad (1)$$

$$= \sum_{s=1}^S x_s(t) a(\theta_s, \phi_s) + \sum_{i=1}^I x_i(t) a(\theta_i, \phi_i) + x_n \quad (2)$$

Where $x_s(t)$, $x_i(t)$, $x_n(t)$, denote the desired signal, interference signal and noise signal added from White Gaussian noise, respectively. The unwanted signal consists of $x_i(t) + x_n(t)$, the desired angle and interference direction of arrival angles are (θ_s, ϕ_s) and (θ_i, ϕ_i) , respectively. $a(\theta_s, \phi_s)$ denote the steering vector for wanted signal while $a(\theta_i, \phi_i)$ refer to the interference signal steering vector.

Steering vector is a complex vector containing responses of all elements from the array to a narrowband source of unit power depending on the incident angle, it is given as [11]:

$$[a(\theta, \phi)]_{N \times M} = \left[\sum_{n=1}^N \sum_{m=1}^M e^{jq(nd_x \cos(\theta) + md_y \sin(\theta) \sin(\phi))} \right] \quad (3)$$

$$A = [a_0, a_1, a_2, \dots, a_{L-1}]^T$$

Where j is the imaginary unit of a complex number, (i.e. $j^2 = -1$), $q = 2\pi/\lambda$ is the wave number, λ is the wavelength of the received signal, (θ, ϕ) composed of azimuth angle $\in [0, 2\pi]$ and elevation angle $\in [0, \pi/2]$ while A denotes the matrix form of the steering vector and $(.)^T$ denote the transposes operators.

The signal $x_T(t)$ received by multiple antenna elements is multiplied by a series of amplitude and phase (weight vector coefficients) which accordingly adjust the amplitude and phase of the incoming signal. This weighted signal is a linear combination of the data at $N \times M$ elements, resulting in the array output, $y(t)$ at any time t , of a narrowband beamformer is given as:

$$y(t) = w_{nm}^H x_T(t) \quad (4)$$

where $y(t)$ is the output of the beamformer, $x_T(t)$ is the output of the antenna elements, w_{nm} is the complex weight vector for the antenna element $= [w_{1,1}, \dots, w_{NM}]^T$ is



$\in \mathbb{C}^{N \times M}$ beamforming complex vector. $(\cdot)^H$ denotes the conjugate transpose (Hermitian transpose) for a matrix.

The weight vector at time $t + 1$ for any system that uses the immediate gradient vector $\nabla J(t)$ for weight vector upgrading and evades the matrix inverse operation can be written as follows:

$$W(t+1) = W(t) + 1/2\mu[\nabla J(t)] \quad (5)$$

where μ is the step size parameter, which controls the speed of convergence and lies between 0 and 1. While the smallest values of μ facilitate the high-quality estimation and sluggish concurrence, the huge values of it may result in a rapid union. However, the constancy over the minimum value may disappear. Consider

$$0 < \mu < 1/\lambda \quad (6)$$

An instantaneous estimation of gradient vector is written as:

$$\nabla J(t) = -2p(t) + 2R(t)W(t) \quad (7)$$

$$p(t) = d^*(t)x_T(t) \quad (8)$$

$$R_y = x_T(t)x_T^H(t) \quad (9)$$

An precise calculation of $\nabla J(t)$ is not possible because prior information on cross-correlation vector, p and covariance matrix, R_y of the measurement vector are required. By substituting (7) into (5), the weight vector is derived as follows:

$$\begin{aligned} W(t+1) &= W(t) + \mu[p(t) - R(t)W(t)] \\ &= W(t) + \mu x_T(t)[d^*(t) - x_T^H(t)W(t)] \\ &= W(t) + \mu x_T e^*(t) \end{aligned} \quad (10)$$

The desired signal can be further defined by the following three formulas:

$$y(t) = w^H(t)x_T(t) \quad (11)$$

$$\begin{aligned} e(t) &= d(t) - y(t) \\ &= W(t) + \mu x_T(t)e^*(t) \end{aligned} \quad (12)$$

The covariance matrix, R_y is constructed conventionally with unlimited snapshots. However, it is estimated by using limited snapshots signal in actual application. It can be expressed as:

$$R_s = \sigma_s^2 a(\theta_s, \phi_s) a^H(\theta_s, \phi_s) \quad (13)$$

$$R_{i+n} = \sum_{i=1}^I \sigma_i^2 a(\theta_i, \phi_i) a^H(\theta_i, \phi_i) + \sigma_n^2 Id_{N \times M} \quad (14)$$

$$R_y = R_s + R_{i+n} = E[x_T(t)x_T^H(t)] \quad (15)$$

where R_y , σ_s^2 , σ_i^2 , σ_n^2 , Id_L , R_s , R_{i+n} and $E[\cdot]$ denotes, respectively, the theoretical covariance matrix, power of the desired signal, interference power, noise power, identity matrix, SOI covariance matrix,

interference plus noise covariance matrix and expectation operator.

The common formulation of the MVDR beamformer that determine the $N \times M$ optimum weight vector is the solution to the following constrained problem [12]:

$$\begin{aligned} \min E[|y(t)|^2] \\ \Rightarrow \min_w P(\theta, \phi) = \{w^H R_y w\} \\ \text{s.t.} \quad w^H a(\theta_s, \phi_s) = 1 \end{aligned} \quad (16)$$

where $P(\theta, \phi)$ denote the mean output power, a beam pattern can be given in dB as [13]:

$$\text{beam pattern} = 20 \log_{10} \frac{|P(\theta, \phi)|}{\max |P(\theta, \phi)|} \quad (17)$$

This technique minimizes the contribution of the undesired signal by minimizing the power of output noise and interference and ensuring the power of useful signal equal to 1 in the real user direction $w^H a(\theta_s, \phi_s) = 1$. By using Lagrange multiplier, the MVDR weight vector that give the solution for above equation as following formula [14]:

$$w_{\text{MVDR}} = \frac{R_y^{-1} a(\theta_s, \phi_s)}{a^H(\theta_s, \phi_s) R_y^{-1} a(\theta_s, \phi_s)} \quad (18)$$

Inserting (19) into (11), the output of MVDR beamformer is given by

$$\begin{aligned} y(t) &= w^H(t)x_T(t) \\ &= w^H a(\theta_s, \phi_s) x_s(t) + w^H x_i(t) a(\theta_i, \phi_i) + w^H x_n \\ &= x_s(t) + w^H x_i(t) a(\theta_i, \phi_i) + w^H x_n \end{aligned} \quad (19)$$

The output signal power from the array as a function of the DOA estimation, using optimum weight vector from MVDR beamforming method [15], it gives by MVDR sp-atial spectrum for angle of arrival estimated by detecting the peaks in this angular spectrum as [16]:

$$P_{\text{MVDR}}(\theta) = \frac{1}{a^H(\theta_s, \phi_s) R_y^{-1} a(\theta_s, \phi_s)} \quad (20)$$

Finally, the SINR defined as;

$$\text{SINR} = 10 \log_{10} \frac{\sigma_s}{\sum_{i=1}^I \sigma_i + \sigma_n} \quad (21)$$

SIMULATION RESULTS AND DISCUSSION

In this paper, $N \times M$ rectangular antenna array (RAAs) configuration arranged along with x-y axis added to the beamformer system at the base station (BS). The array receives signals from different spatially separated users, the received signal at the antenna array consists of desired signal, co-channel interference, and a random noise component. To increase the output power of the desired signal and reduce the power of co-channel interference and noise, beamforming is employed at the BS. The ABF performance analysis shows an array of an even and odd



number of elements separated by inter-element spacing, d , at carrier frequency (F_c) of 2.6 GHz, which is the spectrum band is allocated for LTE operators in Malaysia [17]. To measure the performance of the MVDR algorithm for ABF applications with varying parameters such as the number of elements in the array, distance between the adjacent elements, number of SNOIs, accuracy to distinguish interference in the location very close to the SOI, the number of snapshots (ns), and noise power, σ_n . The goal is to analysis the effect of parameters mentioned above that achieved the best beamforming capabilities to form the main beam in wanted direction and place null in the directions of interference with highest SINR output. Four different scenarios are considered, and the simulation parameters setting in this paper are shown in Table-1.

Table-1. Simulation parameters.

No.	Parameter name	Value
1	Array Type	RAA
2	Antenna	Isotropic
3	F_c	2.6 GHz
4	Number of element ($N \times M$)	6, 9, 16, 25
5	Element spacing ($d_x = d_y = d$)	$\lambda/8, \lambda/4, \lambda/2, \lambda$
6	SNOIs	1, 2, 3, 4
7	Noise power label (σ_n)	-40, -10, 10, 40
8	Snapshots (ns)	10, 50, 250, 500

a) The first scenario

First simulation scenario depicted the results calculated by considered the distance between array elements set to be $d_x = d_y = d = 0.5\lambda$ as usually used in the most MVDR algorithm. Uniform RAA with $N \times M = 6$ isotropic elements of $[N=3, M=2]$, 9 isotropic elements of $[N=3, M=3]$, 16 isotropic elements of $[N=4, M=4]$, and 25 isotropic elements of $[N=5, M=5]$ elements, the additive noise is modeled as a complex zero-mean white Gaussian noise. Three interfering sources are assumed to have Direction of Arrivals (DOAs), $\theta_i \pm 30^\circ$ and 60° with $\phi_i = 0^\circ$ respectively. The desired signal arrival is considered to be a plane wave from the presumed direction ($0^\circ, 0^\circ$). To improve the signal performance of the desired target and nullifying interference directions by using the MVDR BF technique. Figure 2 shows a typical 2D beam pattern plot displayed in the rectangular coordinate, it demonstration the effects if the number of elements is increased for SOI at ($0^\circ, 0^\circ$) and SNOIs at ($\pm 30^\circ, 0^\circ$) and ($60^\circ, 0^\circ$) respectively. This simulation was repeated for 6, 9, 16, and 25 elements with an input SNR of 10dB and 300ns. The plots observe that the MVDR successfully form nulls at each of the income interference sources, and it provide maximum gain to the look direction of the desired user direction. Moreover, increasing the number of elements resulting in the width of the main lobe decreases and the number of nulls in the pattern increases. The number of side lobes (SLs) increases as well the level of the first and subsequent SLs decreases compared to the main lobe. SLs represent power radiated in potentially unwanted directions so in a wireless communications system, SLs will contribute to

the level of interference spread in the cell by a transmitter as well as the level of interference seen by a receiver when antenna arrays are used. The main lobe beamwidth (MLBw), maximum side lobe level (MSLL) that is closest to the main beam, maximum depth null (MDN) at interference direction and output SINR are shown in Table 2. On the other hand, the computing operations become more complex. Besides, as the number of elements increases, the mean cost of design increases due to the increasing number of RF modules, A/D converters, and other components. This causes the operational power consumption to increase too.

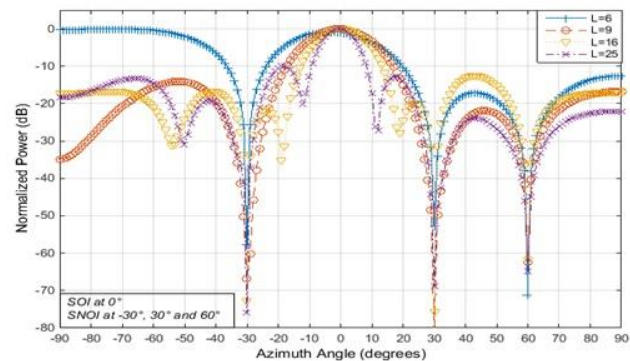


Figure-2. Beam pattern analysis of MVDR varying $N \times M = 6, 9, 16$, and 25 with $d = \lambda/2$.

Table-2. MVDR performance analysis for SOI at 0° and SNOIs at $\pm 30^\circ$ and 60° with varying $N \times M$ at $d = \lambda/2$.

$N \times M$	MLBw [0°]	MSLL [dB]	MDN [dB]	SINR [dB]
6	60°	0.8	-70.2	49.5
9	60°	-14.1	-81.9	54.9
16	38°	-19.9	-75.7	61.0
25	26°	-9.8	-75.9	63.1

b) The second scenario

The distance between the antenna sensors is an important factor in the design of an antenna array. Second simulation scenario illustrates the results that calculated by considering $N=4, M=4$, with interelement spacing of $d_x = d_y = d = \lambda/8, \lambda/4, \lambda/2$, and λ for SOI at ($0^\circ, 0^\circ$) and SNOIs at ($\pm 30^\circ, 0^\circ$) and ($60^\circ, 0^\circ$).

From Figure-3, demonstrates the effect of the element spacing on MVDR performance. It is found that for $\lambda/8$ the power of the main lobe is less than optimum whereas the max power of the main beam achieved by $d = \lambda/4, \lambda/2$, and λ . The coupling effects appear when elements are spaced closely as shown in figure 3 for $d = \lambda/8$ at -90° with a power of 0dB. The side lobe level that is closest to the main beam for each inter-element spacing having a height of ($-0.3, -7.2, -19.9$, and -13.9 at $-90^\circ, -52^\circ, 24^\circ$, and 12°) respectively. Furthermore, if the spacing is less than $\lambda/2$, it does not improve the MVDR performance in terms of resolution, and the coupling effects will be larger and tend to decrease with increasing d . If the spacing is



bigger than $\lambda/2$, causes grating lobes that degrade the MVDR performance also. Therefore, the elements have to be far enough to avoid mutual coupling, and the spacing has to be $\leq \lambda/2$ to avoid grating lobes. As the spacing between elements increases the main beam width decreases resulting in higher directivity, the number of SLs also increases and highest output SINR obtained by $\lambda/2$ due to greatest interference suppression as depicts in Table-3.

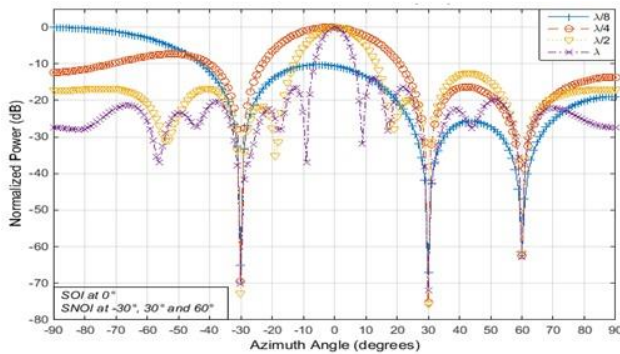


Figure-3. Beam pattern analysis of MVDR varying $d = \lambda/8, \lambda/4, \lambda/2$, and λ with $N \times M = 16$.

Table-3. MVDR performance analysis for SOI at 0° and SNOIs at $\pm 30^\circ$ and 60° with different d and $N \times M = 16$.

$d[m]$	MLBw [0°]	MSLL [dB]	MDN [dB]	SINR [dB]
$\lambda/8$	60°	-0.3	-56.5	48.6
$\lambda/4$	60°	-7.2	-75.2	57.4
$\lambda/2$	38°	-19.9	-75.7	61.0
λ	18°	-13.9	-72.0	61.6

c) The third scenario

Using multiple antennas at the BS can reduce the effects of co-channel interference, multipath fading, and background noise. Many BF algorithms have been devised to cancel interference sources that appear in the cellular system. MVDR algorithm can null the interferences without any distorted to the desired path.

The third simulation scenario demonstrates the MVDR behavior when the number of SNOIs increased. The subsequent MVDR pattern plotted with cancellation for all interferences is shown in Figure-4. It shows a beam pattern for a 16 element rectangular array in the presence of different angle of arrival (AoA) for SOI and SNOIs. In figure-4, the output of MVDR BF algorithm is illustrated against a different number of interference sources as tabulated in Table-4. It can be seen that the performance of the MVDR is affected by the number of SNOIs as the number of interference increases, the SINR decrease. In case of two interference sources, it is found that the deep null of -66.6dB comparing to -48.5dB for 16 elements for a study conduct by [18] based on conjugate gradient method ABF algorithm. For 4 interference sources, the MVDR was able to form the main beam to reach a desired direction even for closest interference to the user which means better

result is obtained when the angular separation between the SOI and SNOI increases.

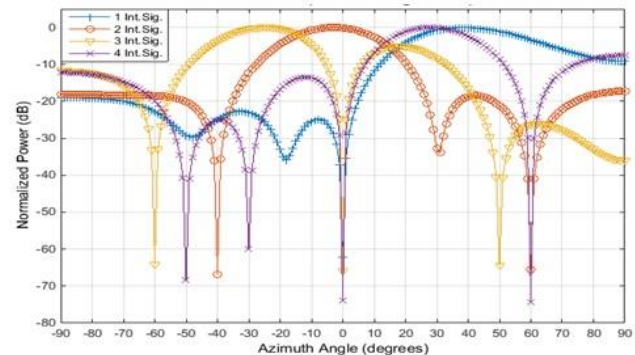


Figure-4. Beam pattern analysis of MVDR, $N \times M = 16$ and $d = \lambda/2$ with different SOI and SNOIs AoAs.

Table-4. Comparison of SINR values for $N \times M = 16$ and $d = \lambda/2$ with different SOI and SNOIs AoAs.

SOI [$^\circ$]	SNOIs [$^\circ$]	MLBw [0°]	MSLL [dB]	MDN [dB]	SINR [dB]
40	0	80°	-9.0	-62.2	62.9
0	-40, 60	70°	-18.3	-66.6	62.2
-20	-60, 0, 50	60°	-4.6	-65.5	59.6
30	-50, -30, 0, 60	60°	-13.3	-74.2	58.9

d) The fourth scenario

In this scenario, compares the effect of various noise power levels, σ_n , and different number of snapshots, n_s , on the performance of MVDR for a desired user at 0° and three interference signal at $\pm 30^\circ$ and 60° with $N=4$, $M=4$, $d=\lambda/2$. Figure-5 give the output beam pattern with four different noise power ranging from -40dB to 40dB. It can be seen that the four curves are noticeably very similar, the MVDR shows better SINR of 92.4dB at a noise power level of -40dB with null all interference sources as demonstrated in Table-5. The output SINR decreases as the noise power increases. However, the reduction (null power) at higher values of σ_n is much less than at lower values of σ_n and the performance of the MVDR algorithm deteriorates as the noise power increases.

Moreover, in Figure-6, the beam pattern of MVDR algorithm for analyzing the performance are illustrated against the number of n_s and compare the output SINR. It can be seen that from this figure that the performance of the MVDR is affected by a number of snapshots where increasing number of n_s resulting in more accurate resolution but also the computational time increases. In terms of required computational time, it is found that the required processing time for MVDR is raising with the snapshot increase as displayed in Table-6. This simulation was operated on Intel® Core 2 Duo CPU @ 3.0GHz, 4GB RAM runs on Windows 7 64bit operating system.

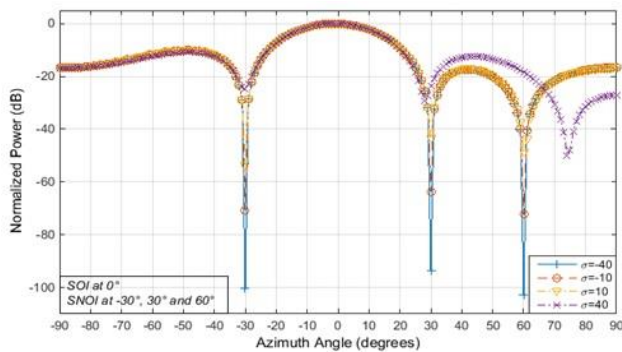


Figure-5. Beam pattern analysis of MVDR varying $\sigma_n = \pm 10$, and ± 40 dB with $N \times M = 16$, $d = \lambda/2$.

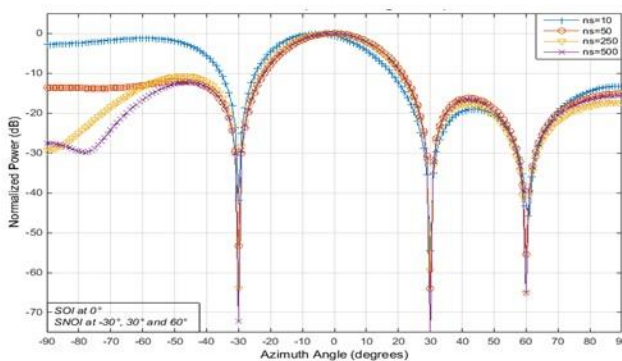


Figure-6. Beam pattern analysis of MVDR varying $n_s = 10, 50, 250$, and 500 with $N \times M = 16$, $d = \lambda/2$.

Table-5. MVDR performance analysis for SOI at 0° and $SNOIs$ at $\pm 30^\circ$ and 60° with different σ_n at $N \times M = 16$ and $d = \lambda/2$.

σ_n [dB]	MLBw [0°]	MSLL [dB]	MDN [dB]	SINR [dB]
-40	60°	-10.0	-102.7	92.4
-10	60°	-10.1	-72.2	62.4
10	60°	-10.3	-53.4	41.9
40	58°	-10.6	-49.9	16.5

Table-6. MVDR performance analysis for SOI at 0° and $SNOIs$ at $\pm 30^\circ$ and 60° with different n_s at $N \times M = 16$ and $d = \lambda/2$.

n_s	MLBw [0°]	MSLL [dB]	MDN [dB]	SINR [dB]	Time [Sec]
10	60°	-0.6	-53.9	38.8	0.87
50	60°	-12.0	-64.0	51.0	1.52
250	60°	-10.7	-64.9	57.3	2.01
500	60°	-12.3	-76.1	64.1	2.63

As seen from Table-5, the main lobe beamwidth (MLBw) remain almost the same and maximum side lobe level (MSLL) slightly change as σ_n increases, while the nulling level and SINR strongly affected with σ_n

increases. In addition, Table-6 shows the SINR increases as n_s increases owing to the increasing probability of finding a better solution. In other words, sharper and deeper nulls would be produced and hence improve the SINR through increasing number of snapshots.

CONCLUSIONS

MVDR adaptive beamforming algorithm with rectangular antenna array geometry has been evaluated in this paper. Different scenario's cases are considered to provide a maximum signal to interference plus noise ratio (SINR) for the desired user direction by placing deepen nulls at directions of the interfere source in the radiation pattern. This paper shows the influence of a different number of antenna elements, different inter element spacing, different number of interference sources with varying angular separations between SOI and interferences, different label of noise power, and different number of snapshots on MVDR beam pattern and SINR. The MVDR beamformer demonstrated its ability to direct the antenna main beam in the direction of the desired user as well as its ability to place null the interference source. The presented results show that when antenna elements are more, the main lobe beamwidth become smaller resulting in higher system capacity. Meanwhile, the drawback is increasing cost, size and complexity. It is found that $\lambda/2$ is the best element spacing [18] for avoiding grating lobes, mutual coupling effects, and better depth null performance. MV-DR rejects with very low power level, and good accuracy can be obtained even in the case of multiple interferences. The noise level is an important factor that affects the MV-DR performance. Increases number of snapshots resulting higher SINR and more accurate main beam pattern. The computation time can be further decreased, if higher signal processor is used. An ongoing research extends the results of this paper to enhanced MVDR.

REFERENCES

- [1] Liberti J. C. and Rappaport T. S. 1999. Smart antennas for wireless communications: IS-95 and third generation CDMA applications. Prentice Hall.
- [2] Garza C. 2011. 4G Digest - 17.25 million BWA/WiMAX and 320 thousand LTE subscribers reached in Q1 2011 in 4G Digest.
- [3] Halim M. A. 2001. Adaptive array measurements in communications. 1st ed. Artech House Publishers. Norwood, MA, USA.
- [4] Pan C., Chen J. and Benesty J. 2014. Performance study of the MVDR beamformer as a function of the source incidence angle. IEEE/ACM Transactions on Audio, Speech, and Language Processing. Vol. 22, No. 1, pp. 67–79.
- [5] Khaldoun A. O. Rahman M. M., Ahmad R. B. and Hassnawi L. A. 2014. Enhanced uniform linear array



- performance using modified minimum variance distortionless response beamformer algorithm, The Second International Conference on Electronic Design (ICED). pp. 198–203.
- [6] Choi R. L.-U., Murch R. D. and Letaief K. 2003. MIMO CDMA antenna system for SINR enhancement. *IEEE Transactions on Wireless Communications*. Vol. 2, No. 2, pp. 240–249.
- [7] Serbetli S. and Yener A. 2004. Transceiver optimization for multiuser MIMO systems. *IEEE Transactions on Signal Processing*. Vol. 52, No. 1, pp. 214–226.
- [8] Manolakis D. G., Ingle V. K. and Kogon S. M. 2005. *Statistical and adaptive signal processing: spectral estimation, signal modeling, adaptive filtering, and array processing*. Artech House, Inc. Norwood, MA, USA.
- [9] Das K. J. and Sarma K. K. 2012. Adaptive Beamforming for Efficient Interference Suppression Using Minimum Variance Distortionless Response. *International Conference on Advancement in Engineering Studies & Technology*. pp. 82–86.
- [10] Gross F. 2015. *Smart antennas with MATLAB: principles and applications in wireless communication*. 2nd ed. McGraw-Hill Professional.
- [11] Allen B. and Ghavami M. 2005. *Adaptive array systems: fundamentals and applications*. John Wiley & Sons.
- [12] Souden M., Benesty J. and Affes S. 2010. A study of the LCMV and MVDR noise reduction filters. *IEEE Transactions on Signal Processing*. Vol. 58, No. 9, pp. 4925–4935.
- [13] Godara L. C. 1997. Application of antenna arrays to mobile communications. II. Beam-forming and direction-of-arrival considerations. *Proceedings of the IEEE*. Vol. 85, No. 8, pp. 1195–1245.
- [14] Renzhou G. 2007. Suppressing radio frequency interferences with adaptive beamformer based on weight iterative algorithm. In *Conference on Wireless, Mobile and Sensor Networks, (CCWMSN07)*, IET.
- [15] Haykin, S. 2013. *Adaptive Filter Theory*. 4th ed. Prentice Hall.
- [16] Capon J. 1969. High-resolution frequency-wavenumber spectrum analysis. *Proceedings of the IEEE*. Vol. 57, No. 8, pp. 1408–1418.
- [17] Malaysian Communications and Multimedia Commission. 2011. *SKMM-MCMC Annual Report*. ; Available from: <http://www.skmm.gov.my/skmmgovmy/media/General/pdf/>.
- [18] Saxena P. and Kothari A. 2014. Performance analysis of adaptive beamforming algorithms for smart antennas. *IERI Procedia, Elsevier*. Vol. 10, pp. 131–137.